HHS Public Access
Author manuscript
J Bone Res. Author manuscript; available in PMC 2023 September 14.

Published in final edited form as:
J Bone Res. 2023 ; 11(4): .

SRT2183 and SRT1720, but not Resveratrol, Inhibit Osteoclast Formation and Resorption in the Presence or Absence of Sirt1

Ramkumar Thiyagarajan,
Maria Rodríguez Gonzalez,
Catherine Zaw,
Kenneth Ladd Seldeen,
Mireya Hernandez,
Manhui Pang,
Bruce Robert Troen

Division of Geriatrics, Department of Internal Medicine, Landon Center on Aging, Kansas University Medical Center, KS and Research Service, Veterans Affairs Kansas City Healthcare System, Kansas City, Missouri, USA

Abstract

Background: Osteoclastic bone resorption markedly increases with aging, leading to osteoporosis characterized by weak and fragile bones. Mice exhibit greater bone resorption and poor bone mass when Sirt1 is removed from their osteoclasts. Here we investigated the *ex vivo* impacts of putative Sirt1 activators, Resveratrol (RSV), SRT2183, and SRT1720, on osteoclast formation and activity in primary mouse bone marrow cells (BMCs) derived from wild-type (WT) and osteoclast specific Sirt1 knockout (OC-Sirt1KO) mice and in the RAW264.7 mouse macrophage cell line.

Results: We found that SRT2183 and SRT1720 inhibit the formation of osteoclasts and actin belts in BMCs and RAW264.7 cells, whereas RSV does not. We also observed that the OC-Sirt1KO mice exhibited less bone mineral density, and the BMCs harvested from these mice yielded more osteoclasts than BMCs harvested from littermate controls. Interestingly, both SRT2183 and SRT1720 reduced osteoclast and actin belt formation in BMCs from OC-Sirt1KO mice. SRT2183 and SRT1720 also significantly disrupted actin belts of mature osteoclasts generated from BMCs of WT mice, within 3 and 6 hours of administration, respectively.

Correspondence to: Bruce Robert Troen, Division of Geriatrics, Department of Internal Medicine, Landon Center on Aging, Kansas University Medical Center, KS and Research Service, Veterans Affairs Kansas City Healthcare System, Kansas City, Missouri, USA, btroen@kumc.edu.

AUTHOR CONTRIBUTIONS
Conceptualization: Manhui Pang, Ramkumar Thiyagarajan, Kenneth Seldeen, Bruce Troen; Investigation: Maria Rodríguez-Gonzalez, Catherine Zaw, Mireya Hernandez, Ramkumar Thiyagarajan; Methodology: Manhui Pang, Ramkumar Thiyagarajan, Bruce Troen; Supervision: Manhui Pang, Kenneth Seldeen, Bruce Troen; Resources: Bruce Troen; Writing-original draft: Ramkumar Thiyagarajan; Writing-review and editing: Ramkumar Thiyagarajan, Kenneth Seldeen, Bruce Troen

COMPETING INTERESTS
All authors have no conflicts of interest.

Furthermore, these compounds inhibited the resorption activity of mature osteoclasts, while RSV did not.

Conclusion: Our findings suggest SRT2183 and SRT1720 impede bone resorption by disrupting actin belts of mature osteoclasts, inhibit actin belt formation, and inhibit osteoclastogenesis even in the absence of Sirt1. Thus, the mechanism of action of these compounds appears to extend beyond Sirt1 activation and possibly pave the way for potential new therapies in alleviating osteoporosis associated bone loss.

Keywords

Osteoporosis; Sirt1; OC-Sirt1KO; Osteoclasts; Actin belts; Bone resorption; Bone marrow cells

INTRODUCTION

More than half of Americans over age 50 will be at risk for an osteoporosis associated fracture, a leading cause of morbidity and mortality in older individuals [1]. Sirtuin (Sirt1), a nicotinamide adenine dinucleotide dependent deacetylase, is known to increase the health span and lifespan and delay the onset of many aging-related diseases in mice [2–10], and also appears to increase bone mass [11]. Young mice without Sirt1 in their osteoclasts exhibit greater bone resorption and diminished Bone Mineral Density (BMD) [11,12]. Resveratrol (RSV), a natural polyphenol/phytoalexin, increases Sirt1 expression and life span in yeast, C. *elegans*, and drosophila [8–10]. Mice treated with RSV exhibit greater bone mineral density, bone strength, and trabecular thickness [13]. In addition, RSV treated osteoporotic rats show increased bone mineral density and bone strength, as well as reduced femoral porosity compared to untreated osteoporotic counterparts [14]. SRT1720 and SRT2183 are structurally different from RSV, but were designed specifically to activate Sirt1, and both compounds impact bone metabolism [11,15,16]. Treatment of middle-aged male mice and young ovariectomized female mice with SRT1720 increases bone volume [11]. Further, Gurt et al. [15], showed that *ex vivo* treatment with SRT2183 of Bone Marrow Cells (BMCs) from 8-week-old female 129/Sv mice inhibits osteoclast formation and diminishes bone resorption activity, and used constitutive Sirt1 knockout mice (lacking Sirt1 exons 5, 6 and 7) to demonstrate the role of Sirt1 on osteoclastogenesis [15]. However, the mode of action of these compounds remains poorly elucidated. Previous studies involving various biochemical assays and biophysical tests have revealed that RSV, SRT2183, and SRT1720 act on targets other than Sirt1 [17,18]. Thus, we investigated the impact of RSV, SRT2183, and SRT1720 upon osteoclast formation and resorption in BMCs from skeletally mature (4 to 6-month-old) male WT C57BL6 mice. In addition, in order to test to impact of Sirt1 in osteoclasts formation, we utilized a mouse model that lacks the Sirt1 catalytic domain (exon 4 $Sirt1^{exon4^{-/-}}$) specifically in osteoclast precursors [12]. We found that the SRT2183 and SRT1720 consistently inhibit osteoclastogenesis and actin belt formation independent of the presence of intact Sirt1. Furthermore, SRT2183 and SRT1720 significantly disrupt actin belts and inhibit resorption activity of mature osteoclasts.

MATERIALS AND METHODS

Mice

All studies and experimental protocols were approved by and complied with the guidelines of the Miami VA Animal Care and Use Committee, the University at Buffalo, and the VA Western New York Institutional Animal Care and Use Committees. Mice were maintained under a 12-hour light and 12-hour dark cycle and at all times provided *ad libitum* access to chow and water. The osteoclast specific Sirt1$^{exon4-/-}$ (OC-Sirt1KO) mice were a gift from Dr. James Edwards [12], and the mice line was maintained in our facility. In order to maintain the colony, the mice with exon 4 mutation were mated with mice expressing the Cre recombinase, specifically in osteoclasts (driven by the lysozyme M promoter). Primary BMCs were collected from 4-month-old male littermate controls or OC-Sirt1KO mice (C57BL/6J).

Reagents

Resveratrol was purchased from Sigma-Aldrich (St. Louis, MO). SRT1720, and SRT2183 were purchased from Calbiochem (San Diego, CA), and Selleckchem (Houston, TX), respectively. Soluble mouse RANKL was acquired from Santa Cruz Biotechnology (Santa Cruz, CA). Recombinant mouse M-CSF (mM-CSF) was obtained from R and D Systems (Minneapolis, MN). High glucose alpha-MEM (α-MEM) and 100X penicillin G/streptomycin were purchased from Life Technologies/Invitrogen (Grand Island, NY). Fetal Bovine Serum (FBS) was from Thermo Fischer Scientific/Hyclone (Logan, UT). All other reagents used in this study were from Sigma-Aldrich.

Bone mineral density measurement

Bone Mineral Density (BMD) was measured by Dual-Energy X-ray Absorptiometry (DEXA) using a Lunar PIXImus II (Inside Outside Sales, LLC, Fitchburg, Wisconsin). The OC-Sirt1KO male mice and littermate control mice (n=6) were anesthetized with an intraperitoneal injection of ketamine and xylazine (100 mg/kg and 20 mg/kg mouse, respectively). Then DEXA analysis was performed as a single scan.

Primary BMC isolation

BMCs isolated from C57BL/6J mice were used for bone marrow macrophage and osteoclast differentiation. Briefly, BMCs were flushed from the tibiae and femorae. After the lysis of red blood cells, the BMCs were plated in a 10 cm tissue culture dish with α-MEM complete medium (basal α-MEM medium supplemented with 10% FBS, 100 U/ml penicillin G, and 100 μg/ml streptomycin and 2 mM glutamine) and 20 ng/ml mM-CSF (macrophage/monocyte colony stimulating factor). After overnight incubation in a humidified atmosphere of 5% CO_2 at 37°C, the non-adherent BMCs were collected for further experimentation.

RAW264.7 cell culture

RAW264.7 cells were purchased from American Type Culture Collection (ATCC, Manassas, VA). The RAW264.7 cells were maintained in high glucose D-MEM complete medium (basal D-MEM supplemented with 10% fetal bovine serum, 100 U/ml penicillin G, and

100 μg/ml streptomycin and 2 mM glutamine), and in a humidified atmosphere of 5% CO_2 at 37°C. Cells were maintained in suspension culture in non-coated petri dishes (Greiner Bio-one, Monroe, NC), which markedly reduces drift toward a differentiated state, and for experiments cells were plated on standard tissue culture dishes.

Cell viability assay

After overnight incubation with 20 ng/ml mM-CSF, the non-adherent BMCs were collected and plated as 1×10^5 cells/0.25 ml/well in a 96-well plate with 20 ng/ml mM-CSF and 40 ng/ml RANKL in the presence or absence of RSV, SRT2183, and SRT1720 for 3 days. Similarly, RAW264.7 cells were plated as 1000 cells/0.25ml/well in a 96-well plate with 40 ng/ml RANKL in the presence or absence of RSV, SRT2183, and SRT1720 for 3 days. After 3 days, cell viability was assessed using Vybrant® MTT Cell Proliferation Assay Kit (Thermo Fischer Scientific, Grand Island, NY) following the manufacturer's protocol. Briefly, 12 mM MTT (3-(4,5-dimethylthiazol-2-yl)-2,5-diphenyltetrazolium bromide) is added to the cells, which is then converted to insoluble formazan. The insoluble formazan was solubilized using an SDS-HCl solution, and the concentration was determined by measuring optical density at 570 nm.

Osteoclast differentiation and visualization of osteoclasts and actin belts

The non-adherent cells were resuspended in a-MEM complete medium, containing 20 ng/ml mM-CSF and 40 ng/ml RANKL, and subsequently cultured in 24-well plates at a density of 5×10^5 cells per well, the presence or absence of RSV, SRT2183, and SRT1720. The medium was replaced every 2–3 days with fresh mM-CSF and RANKL for 6–7 days. The RAW264.7 cells were cultured in a 48-well plate at a density of 4×10^3 per well and were differentiated with 40 ng/ml of RANKL in a-MEM complete medium for 3–4 days. The differentiated osteoclasts were fixed and stained either with a Tartrate Resistance Acid Phosphatase (TRAP) kit (Sigma-Aldrich) to visualize osteoclasts or FITC-phalloidin to visualize actin belts. The TRAP-positive multinucleated osteoclasts (≥ 3 nuclei) were counted manually.

Disruption of actin belts of mature osteoclasts

After 6–7 days of differentiation of BMCs or 3–4 days of differentiation of RAW264.7 to osteoclasts, the mature osteoclasts were treated with vehicle (0.1% DMSO), RSV, SRT2183, or SRT1720 for 3 and 6 hours. After the 3 or 6-hour time points, the actin belts of mature osteoclasts were fixed and visualized with FITC-phalloidin.

Resorption pit assay on cortical bovine bone slices

On day 7, mature osteoclasts were lifted off the plate, using accutase solution (Sigma-Aldrich) and reseeded on cortical bovine bone slices (Boneslices.com, Jelling, Denmark) at a density of 5×10^4 cells per bone slice (6 mm diameter and 0.4 mm thickness) in a 96 well plate. The osteoclasts were cultured in a-MEM complete media, containing 20 ng/ml mM-CSF, 40 ng/ml RANKL and with or without RSV, SRT2183, and SRT1720. After 3 days, the cells were removed using cotton swabs, and the resorption pits were visualized with 0.1% toluidine blue and quantified with ImageJ software [19].

Cell lysate preparation and western blotting

Following various treatments, BMCs or osteoclasts were washed with cold PBS and lysed in cold RIPA buffer. Lysates were kept on ice and vortexed for 15 seconds, every 10 min, three times. Cell lysates were centrifuged at 17,000 g for 15 min at 4°C, and the supernatants were collected. Pierce Bicinchoninic Acid (BCA) protein assay solution (Thermo Fischer Scientific, Grand Island, NY) was added to supernatants and protein standards. Then the protein concentration was measured using a standard plate reader (Bio-Rad Laboratories Ltd., Hercules, CA) at 560 nm. Approximately 30 μg of protein were separated on an 8% SDS-PAGE and electro-transferred to a PVDF membrane. Membranes were blocked in 5% milk in tris-buffered saline with 0.05% Tween 20 for 1 hour at room temperature and then incubated overnight with anti-Sirt1 antibody (07–131, Millipore, Burlington, MA) or anti-AMPKα (AMP-activated protein kinase-alpha, 2603, Cell Signaling Technology, Danvers, MA) or anti-phosphorylated AMPKα (2535, Cell Signaling Technology, Danvers, MA) at 4°C. The next day, the membrane was washed with TBST and incubated with horseradish peroxidase-conjugated secondary antibody (1:5000) for 1 hour at room temperature. Protein bands were detected by chemiluminescence using Pierce™ ECL western blotting substrate (Thermo Fischer Scientific, Grand Island, NY). GAPDH (ab181602, Abcam, Cambridge, UK) was used as the reference protein.

Data analysis

Data are expressed as mean ± SD. One-way ANOVA and post hoc Tukey's multiple comparisons test were applied to analyze differences between vehicle control, RSV, SRT2183, and SRT1720 treatments using GraphPad software. Comparisons between WT and Sirt1KO mice were performed using an unpaired Student's T-Test. P-values of <0.05 were considered statistically significant.

RESULTS

SRT2183 and SRT1720 inhibit osteoclast and actin belt formation, while RSV does not

We assessed the viability of the BMCs and RAW264.6 cells with various concentrations of the compounds: SRT2183 (1 μM and 5 μM), SRT1720 (0.3 μM, 0.6 μM, and 1.2 μM), and RSV (1 μM, 5 μM, and 12.5 μM). We did not notice a significant decline in cell density at any concentrations, except RSV at 12.5 μM impaired BMC viability by 60% (Supplementary Figure 1A), whereas, in RAW264.7 cells, 10 μM RSV and 1.2 μM SRT1720 reduced cell viability by more than 90% and 70%, respectively (Supplementary Figure 1B). Therefore, we used a concentration of 5 μM SRT2183, 0.6 μM SRT1720, and 5 μM RSV on both BMCs and RAW264.7 cells.

The 5 μM RSV did not impede RANKL induced osteoclast formation in primary BMCs (Figures 1A and 1B) and RAW264.7 cells (Supplementary Figures 2A and 2B). In contrast to RSV, SRT2183 (5 μM) and SRT1720 (0.6 μM) markedly inhibited the osteoclastogenesis in a dose-dependent manner (Figures 1A and 1B) without affecting viability (Supplementary Figures 1A and 1B). We further examined whether these compounds altered actin belt formation, essential for bone resorption. Both SRT2183 and SRT1720 significantly inhibited

actin belt formation in BMCs and RAW264.7 cells (Supplementary Figures 2C and 2D), while RSV did not inhibit actin belt formation (Figures 2A and 2B).

Osteoclasts specific Sirt1 knockout (OC-Sirt1KO) mice exhibit low bone mineral density

It is reported that Sirt1 plays an important role in osteoclastogenesis [11,15,20]. In order to understand the impact of Sirt1 on bone, we utilized transgenic mice with osteoclast specific ablation of the Sirt1 exon4, which comprises the catalytic domain that confers Sirt1 deacetylase activity [21]. Using immunoblotting, we confirmed the absence of full-length Sirt1 protein using immunoblotting (Figure 3A).

The OC-Sirt1KO mice exhibited decreased bone mineral density (BMD: 52.2 ± 0.6 mg/cm2 *vs.* 55.6 ± 2.7 mg/cm2, p=0.0213) compared to WT littermate controls (Figure 3B). Further, BMCs harvested from OC-Sirt1KO mice exhibited markedly increased osteoclastogenesis (p<0.001) than did those from the littermate controls (Figures 3C and 3D).

SRT2183 and SRT1720 inhibit osteoclast and actin belt formation in BMCs derived from osteoclast specific Sirt1KO (OC-Sirt1KO) mice

We therefore set out to determine whether Sirt1 mediated the impacts of SRT2183 and SRT1720 inhibition of osteoclast formation. Interestingly, both SRT2183 and SRT1720 significantly inhibited osteoclastogenesis in BMCs from the OC-Sirt1KO mice, whereas RSV did not (Figures 4A and 4B). Furthermore, SRT2183 and SRT1720 markedly suppressed actin belt formation in BMCs harvested from OC-Sirt1KO mice, whereas again RSV did not (Figures 4C and 4D).

SRT2183 and SRT1720 disrupt actin belts of mature osteoclasts and prevent bone resorption, while RSV does not

Since actin belts are required for bone resorption by mature osteoclasts and SRT2183 and SRT1720 significantly inhibit actin belt formation and osteoclastogenesis, we set out to assess the impacts of these compounds on mature osteoclasts. We found that both SRT2183 and SRT1720 disrupted actin belts in mature osteoclasts within 3 and 6 hours after treatment, respectively (Figure 5A). Similarly, in RAW264.7 cells, SRT2183 disrupted actin belts at 3 hours, while SRT1720 took 30 hours to completely disrupt actin belts of mature osteoclasts (Supplementary Figure 3). We next set out to assess whether the disruption of actin belts of mature osteoclasts by these compounds affected osteoclastic bone resorption. We reseeded mature osteoclasts on bovine cortical bone slices and then treated with RSV, SRT2183 and SRT1720 for 72 hours, to provide sufficient time for resorption. We found that the SRT2183 (p<0.001) and SRT1720 (p<0.001) significantly diminished resorption pits (eroded area) on bone slices, while RSV increased bone resorption (p=0.037) (Figures 5B and 5C).

DISCUSSION

During osteoporosis, osteoclastic bone resorption overwhelms bone formation leading to loss of bone mass and increased fragility [22]. Dynamic bone resorption requires mature osteoclasts with intact actin belts. Here we examined the role of Sirt1 activators (RSV,

SRT2183 and SRT1720) on osteoclastic bone resorption, *ex vivo*. We found that SRT2183 and SRT1720 inhibit the formation of osteoclasts and actin belts in primary BMCs derived from WT and OC-Sirt1KO mice, while RSV does not. We also observed that SRT2183 and SRT1720 inhibit bone resorption by disrupting the actin belts of mature osteoclasts. Our findings contrast with previous studies that showed reduced osteoclast formation with RSV treatment in various cell types, such as monocytes from human peripheral blood mononuclear cells, primary bone-derived cells from canine bone fragments, and RAW264.7 cells [23–26]. To our knowledge, no previous *ex vivo* studies have shown the effect of RSV on osteoclastogenesis in mouse primary BMCs, although previous studies demonstrated a positive impact on osteogenesis and osteoblast formation [27,28]. We chose a 5 μM concentration of RSV based on our cell viability assay data. To our surprise, 5 μM RSV did not reduce osteoclastogenesis and instead appears to increase osteoclast formation in either BMCs or RAW264.7 cells. In contrast, He et al. showed that 3 μM RSV reduced osteoclastogenesis in RAW264.7 cells [25]. We note that although RSV did not inhibit osteoclast and actin belt formation in our experiments, it increased phosphorylation of AMPK-α (Supplementary Figure 4) in both BMMs and RAW264.7 cells, which indicates that RSV activated Sirt1, consistent with previous reports [29,30]. Thus, the differences between our findings and those of He et al. may be due to the number of RAW264.7 cells plated (20,000 cells *vs.* 12,500 cells per well) and the concentration of RANKL used to differentiate RAW264.7 cells to osteoclasts (40 ng/ml of RANKL *vs.* 3 ng/ml of RANKL) [25].

However, we observed that both SRT2183 and SRT1720 significantly inhibit RANKL induced differentiation of primary BMCs from young male mice and RAW264.7 cells to osteoclasts. To our knowledge, no studies have tested the *ex vivo* effect of SRT1720 on osteoclastogenesis in primary BMCs. Nevertheless, a recent *in vivo* study by Zainabadi et al. [11], demonstrated that SRT1720 treatment improved bone health in middle-aged male mice and in ovariectomized female mice. Furthermore, consistent with our findings, Gurt et al. [15], observed fewer osteoclasts after treatment of primary BMCs harvested from 8-week-old female 129/Sv mice with 1 μM SRT2183 *ex vivo*.

As Sirt1 is known to regulate bone mineral metabolism, we studied osteoclasts generated from BMCs harvested from osteoclast specific Sirt1 knockout (OC-Sirt1KO) mice. We found that OC-Sirt1KO mice exhibited less bone mineral density, and BMCs harvested from these mice yielded more osteoclasts as compared to WT mice. In support of these observations, previous studies have also observed poor bone mass and greater osteoclastogenesis in OC-Sirt1KO mice as compared to the littermate controls [11,12]. This supports a role for Sirt1 in osteoclastogenesis. Surprisingly, although SRT2183 and SRT1720 are considered Sirt1 activating compounds [31–33], both of these agents inhibited osteoclast and actin belt formation in BMCs harvested from the OC-Sirt1KO male mice. These findings are consistent with the previous study by Gurt et al. [15], showing that SRT2183 inhibits osteoclast formation and resorption activity in BMCs from constitutive Sirt1 knockout female mice. In addition, Huber et al. [17], and Pacholec et al. [18], demonstrated Sirt1 independent effects of SRT2183 and SRT1720 on mouse embryonic fibroblasts and human bone osteosarcoma epithelial cells (U2OS), but did not examine on BMCs or osteoclasts. In contrast, studies have also demonstrated Sirt1-dependent beneficial

impacts of these Sirt1 activating compounds [5,34]. Our *in vivo* data shows that Sirt1 may take part in bone mineral metabolism by altering BMD in OC-Sirt1KO mice, but Sirt1 is not required for inhibiting actin belt organization and osteoclastogenesis *ex vivo* by SRT2183 or SRT1720.

Organized actin rings form a stable actin belt in mature osteoclasts, which is an important factor for osteoclastic bone resorption. Actin belts generate a sealing zone under which energy consuming dynamic bone resorption occurs [35], and it has been shown that the targeted disruption of genes responsible for actin cytoskeleton organization lead to poor bone resorption [36,37]. In our study, SRT2183 and SRT1720 consistently disrupted the actin belts of mature osteoclasts and efficiently inhibited resorption pit formation in cortical bovine bone slices. Gurt et al. [15], also demonstrated poor pit formation by SRT2183 treated osteoclasts derived from mouse BMCs.

CONCLUSION

Our results indicate that both SRT2183 and SRT1720 inhibit osteoclast and actin belt formation in primary BMCs harvested from both WT and OC-Sirt1KO mice, while RSV does not. These Sirt1 activating compounds, therefore, can act independent of Sirt1. Furthermore, SRT2183 and SRT1720 efficiently inhibit bone resorption by disrupting the actin belts of mature osteoclasts. Therefore, SRT2183 and SRT1720 likely act *via* additional pathways to inhibit osteoclast formation and bone resorption.

Supplementary Material

Refer to Web version on PubMed Central for supplementary material.

ACKNOWLEDGEMENT

Research supported by Indian Trail Foundation, VA Merit Review (BX000758), and the Department of Medicine, Jacobs School of Medicine and Biomedical Sciences, University at Buffalo. We thank Dr. Kent Søe, Associate Professor, Clinical Cell Biology, Department of Pathology, Odense University Hospital, University of Southern Denmark, 5000 Odense C, Denmark, for providing valuable suggestions on the analysis of resorption pits in bovine bone slices.

FUNDING

Supported by VA BLRD (BX000758), NIH (K07-AG060266), and the Indian Trail Foundation.

Abbreviations:

BMC	Bone Marrow Cell
BMD	Bone Mineral Density
DMSO	Dimethy Sulfoxide
KO	Knock Out
OC	Osteoclast
RSV	Resveratrol

Sirt	Sirtuin
WT	Wild Type

REFERENCES

1. Office of the Surgeon General (US). Bone health and osteoporosis: A report of the surgeon general 2004.
2. Dali-Youcef N, Lagouge M, Froelich S, Koehl C, Schoonjans K, Auwerx J. Sirtuins: The 'magnificent seven', function, metabolism and longevity. Ann Med 2007;39(5):335–345. [PubMed: 17701476]
3. Mitchell SJ, Martin-Montalvo A, Mercken EM, Palacios HH, Ward TM, Abulwerdi G, et al. The SIRT1 activator SRT1720 extends lifespan and improves health of mice fed a standard diet. Cell Rep 2014;6(5):836–843. [PubMed: 24582957]
4. Satoh A, Brace CS, Rensing N, Cliften P, Wozniak DF, Herzog ED, et al. Sirt1 extends life span and delays aging in mice through the regulation of Nk2 homeobox 1 in the DMH and LH. Cell Metab 2013;18(3):416–430. [PubMed: 24011076]
5. Mercken EM, Mitchell SJ, Martin-Montalvo A, Minor RK, Almeida M, Gomes AP, et al. SRT 2104 extends survival of male mice on a standard diet and preserves bone and muscle mass. Aging Cell 2014;13(5):787–796. [PubMed: 24931715]
6. Banks AS, Kon N, Knight C, Matsumoto M, Gutiérrez-Juárez R, Rossetti L, et al. SirT1 gain of function increases energy efficiency and prevents diabetes in mice. Cell Metab 2008;8(4):333–341. [PubMed: 18840364]
7. Baur JA, Pearson KJ, Price NL, Jamieson HA, Lerin C, Kalra A, et al. Resveratrol improves health and survival of mice on a high-calorie diet. Nature 2006;444(7117):337–42. [PubMed: 17086191]
8. Howitz KT, Bitterman KJ, Cohen HY, Lamming DW, Lavu S, Wood JG, et al. Small molecule activators of sirtuins extend Saccharomyces cerevisiae lifespan. Nature 2003;425(6954):191–196. [PubMed: 12939617]
9. Rogina B, Helfand SL. Sir2 mediates longevity in the fly through a pathway related to calorie restriction. Proc Natl Acad Sci 2004;101(45):15998–6003. [PubMed: 15520384]
10. Wood JG, Rogina B, Lavu S, Howitz K, Helfand SL, Tatar M, et al. Sirtuin activators mimic caloric restriction and delay ageing in metazoans. Nature 2004;430(7000):686–689. [PubMed: 15254550]
11. Zainabadi K, Liu CJ, Caldwell AL, Guarente L. SIRT1 is a positive regulator of in vivo bone mass and a therapeutic target for osteoporosis. PLoS One 2017;12(9):e0185236. [PubMed: 28937996]
12. Edwards JR, Perrien DS, Fleming N, Nyman JS, Ono K, Connelly L, et al. Silent information regulator (Sir) T1 inhibits NF-κB signaling to maintain normal skeletal remodeling. J Bone Miner Res 2013;28(4):960–9. [PubMed: 23172686]
13. Pearson KJ, Baur JA, Lewis KN, Peshkin L, Price NL, Labinskyy N, et al. Resveratrol delays age-related deterioration and mimics transcriptional aspects of dietary restriction without extending life span. Cell Metab 2008;8(2):157–168. [PubMed: 18599363]
14. Wang X, Chen L, Peng W. Protective effects of resveratrol on osteoporosis via activation of the SIRT1-NF-κB signaling pathway in rats. Exp Ther Med 2017;14(5):5032–5038. [PubMed: 29201210]
15. Gurt I, Artsi H, Cohen-Kfir E, Hamdani G, Ben-Shalom G, Feinstein B, et al. The Sirt1 activators SRT2183 and SRT3025 inhibit RANKL-induced osteoclastogenesis in bone marrow-derived macrophages and down-regulate Sirt3 in Sirt1 null cells. PLoS One 2015;10(7):e0134391. [PubMed: 26226624]
16. Milne JC, Lambert PD, Schenk S, Carney DP, Smith JJ, Gagne DJ, et al. Small molecule activators of SIRT1 as therapeutics for the treatment of type 2 diabetes. Nature 2007;450(7170):712–716. [PubMed: 18046409]
17. Huber JL, McBurney MW, DiStefano PS, McDonagh T. SIRT1-independent mechanisms of the putative sirtuin enzyme activators SRT1720 and SRT2183. Future Med Chem 2010;2(12):1751–1759. [PubMed: 21428798]

18. Pacholec M, Bleasdale JE, Chrunyk B, Cunningham D, Flynn D, Garofalo RS, et al. SRT1720, SRT2183, SRT1460, and resveratrol are not direct activators of SIRT1. J Biol Chem 2010;285(11):8340–8351. [PubMed: 20061378]
19. Schneider CA, Rasband WS, Eliceiri KW. NIH Image to ImageJ: 25 years of image analysis. Nat Methods 2012;9(7):671–675. [PubMed: 22930834]
20. Kim HN, Han L, Iyer S, de Cabo R, Zhao H, O'Brien CA, et al. Sirtuin1 suppresses osteoclastogenesis by deacetylating FoxOs. Mol Endocrinol 2015;29(10):1498–1509. [PubMed: 26287518]
21. Cheng HL, Mostoslavsky R, Saito SI, Manis JP, Gu Y, Patel P, et al. Developmental defects and p53 hyperacetylation in Sir2 homolog (SIRT1)-deficient mice. Proc Natl Acad Sci 2003;100(19):10794–10799. [PubMed: 12960381]
22. Feng X, McDonald JM. Disorders of bone remodeling. Annu Rev Pathol 2011;6:121145.
23. Boissy P, Andersen TL, Abdallah BM, Kassem M, Plesner T, Delaissé JM. Resveratrol inhibits myeloma cell growth, prevents osteoclast formation, and promotes osteoblast differentiation. Cancer Res 2005;65(21):9943–9952. [PubMed: 16267019]
24. Feng YL, Jiang XT, Ma FF, Han J, Tang XL. Resveratrol prevents osteoporosis by upregulating FoxO1 transcriptional activity. In J Mol Med 2018;41(1):202–212.
25. He X, Andersson G, Lindgren U, Li Y. Resveratrol prevents RANKL-induced osteoclast differentiation of murine osteoclast progenitor RAW 264.7 cells through inhibition of ROS production. Biochem Biophys Res Commun 2010;401(3):356–362. [PubMed: 20851107]
26. Shakibaei M, Buhrmann C, Mobasheri A. Resveratrol-mediated SIRT-1 interactions with p300 modulate receptor activator of NF-κB ligand (RANKL) activation of NF-κB signaling and inhibit osteoclastogenesis in bone-derived cells. J Biol Chem 2011;286(13):11492–1505. [PubMed: 21239502]
27. Wang W, Zhang LM, Guo C, Han JF. Resveratrol promotes osteoblastic differentiation in a rat model of postmenopausal osteoporosis by regulating autophagy. Nutr Metab 2020;17(1):29.
28. Wei L, Chai S, Yue C, Zhang H, Li J, Qin N. Resveratrol protects osteocytes against oxidative stress in ovariectomized rats through AMPK/JNK1-dependent pathway leading to promotion of autophagy and inhibition of apoptosis. Cell Death Discov 2023;9(1):16. [PubMed: 36681672]
29. Price NL, Gomes AP, Ling AJ, Duarte FV, Martin-Montalvo A, North BJ, et al. SIRT1 is required for AMPK activation and the beneficial effects of resveratrol on mitochondrial function. Cell Metab 2012;15(5):675–690. [PubMed: 22560220]
30. Lan F, Weikel KA, Cacicedo JM, Ido Y. Resveratrol-induced AMP-activated protein kinase activation is cell-type dependent: lessons from basic research for clinical application. Nutrients 2017;9(7):751. [PubMed: 28708087]
31. Feige JN, Lagouge M, Canto C, Strehle A, Houten SM, Milne JC, et al. Specific SIRT1 activation mimics low energy levels and protects against diet-induced metabolic disorders by enhancing fat oxidation. Cell Metab 2008;8(5):347–358. [PubMed: 19046567]
32. Smith JJ, Kenney RD, Gagne DJ, Frushour BP, Ladd W, Galonek HL, et al. Small molecule activators of SIRT1 replicate signaling pathways triggered by calorie restriction in vivo. BMC Syst Biol 2009;3(1):31. [PubMed: 19284563]
33. Yamazaki Y, Usui I, Kanatani Y, Matsuya Y, Tsuneyama K, Fujisaka S, et al. Treatment with SRT1720, a SIRT1 activator, ameliorates fatty liver with reduced expression of lipogenic enzymes in MSG mice. Am J Physiol Endocrinol Metab 2009;297(5):E1179–E1186. [PubMed: 19724016]
34. Hubbard BP, Gomes AP, Dai H, Li J, Case AW, Considine T, et al. Evidence for a common mechanism of SIRT1 regulation by allosteric activators. Science 2013;339(6124):1216–1219. [PubMed: 23471411]
35. Saltel F, Chabadel A, Bonnelye E, Jurdic P. Actin cytoskeletal organisation in osteoclasts: A model to decipher transmigration and matrix degradation. Eur J Cell Biol 2008;87(8–9):459–468. [PubMed: 18294724]
36. Lowe C, Yoneda T, Boyce BF, Chen H, Mundy GR, Soriano P. Osteopetrosis in Src-deficient mice is due to an autonomous defect of osteoclasts. Proc Natl Acad Sci 1993;90(10):4485–4489. [PubMed: 7685105]

37. Soriano P, Montgomery C, Geske R, Bradley A. Targeted disruption of the c-src proto-oncogene leads to osteopetrosis in mice. Cell 1991;64(4):693–702. [PubMed: 1997203]

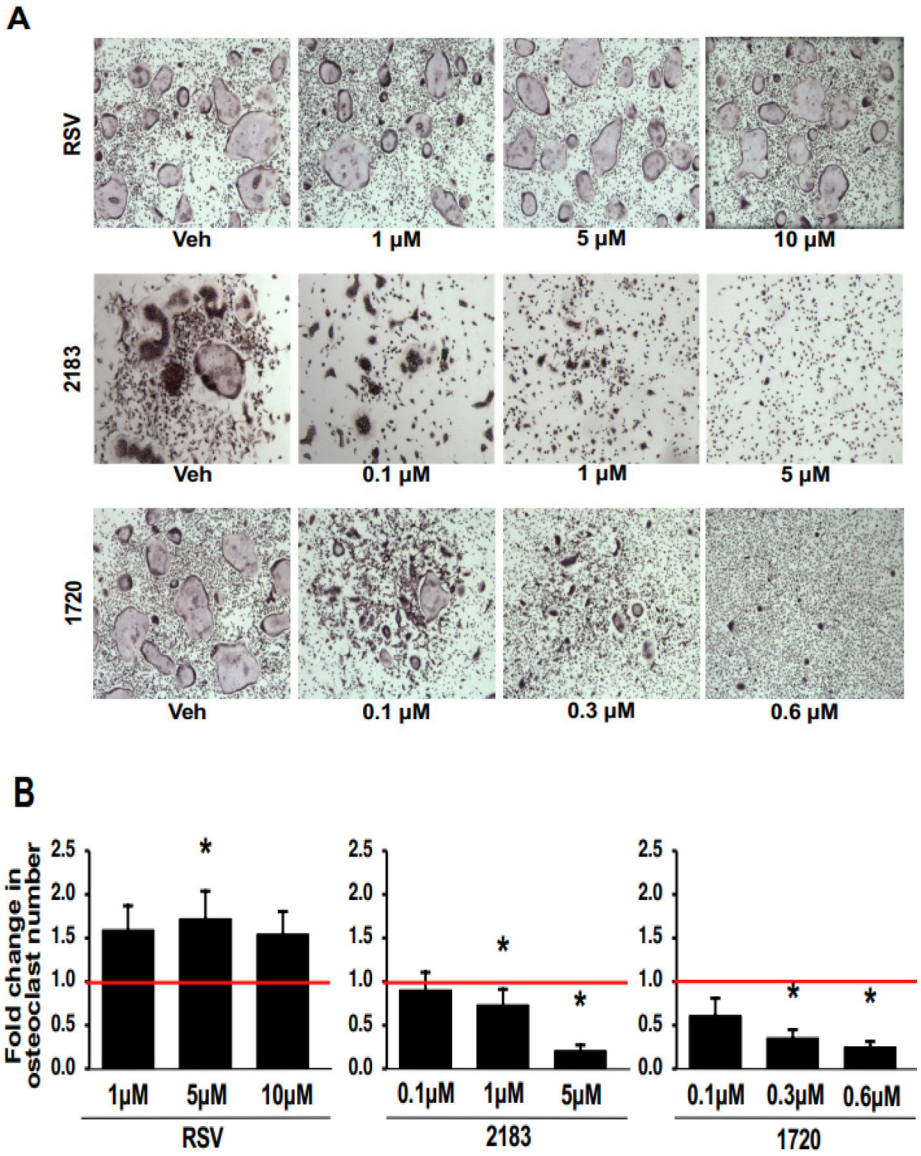

Figure 1:

SRT2183 and SRT1720 inhibit osteoclast formation in BMCs from WT mice, while RSV does not (A) TRAP staining of RSV, SRT2183, and SRT1720 treated multi-nuclear osteoclasts in the presence of M-CSF (20 ng/ml) and RANKL (40 ng/ml). (B) Osteoclasts with 3 or more nuclei were counted, and the values are represented in fold change compared to vehicle (MCSF+RANKL) control (red line). Three independent experiments were performed with ≥ 3 wells per condition. **Note:** * $p<0.05$, compared with WT vehicle control. Data expressed as mean ± SD.

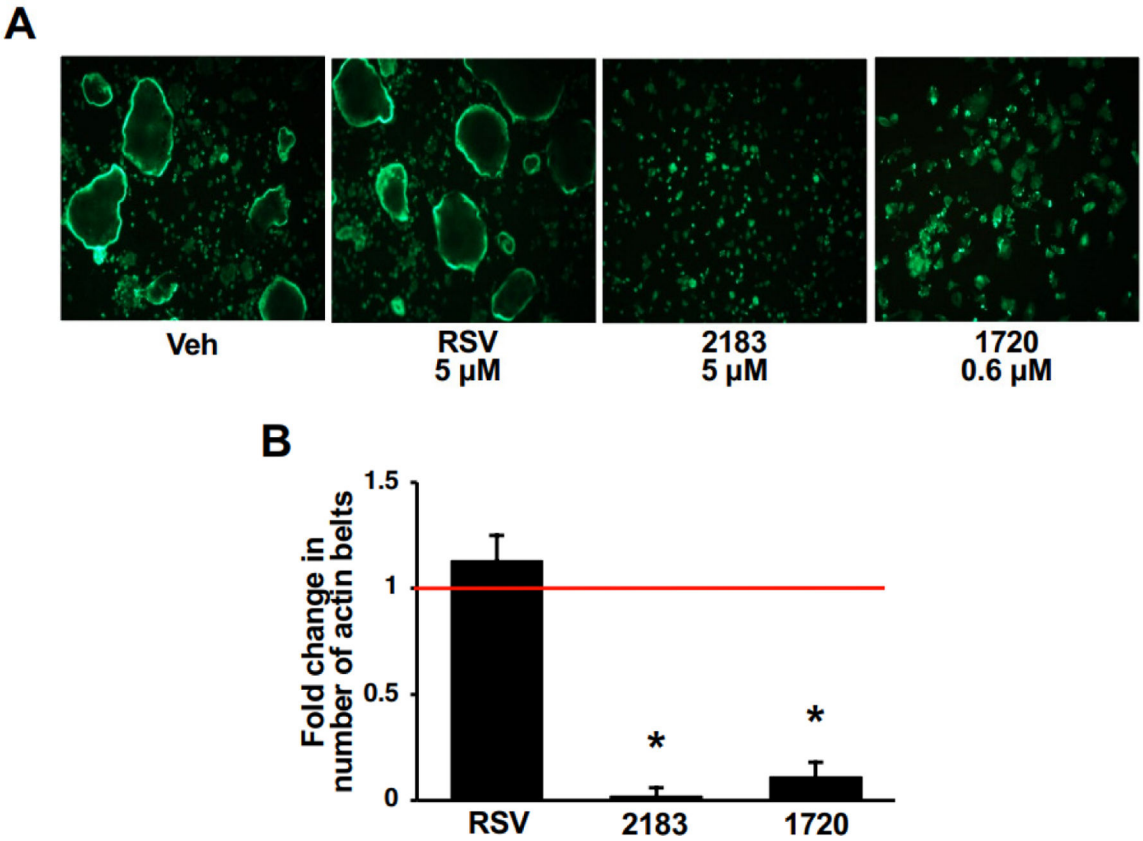

Figure 2:

SRT2183 and SRT1720 disrupt actin belt formation in BMCs from WT mice, while RSV does not (A) Primary mouse BMCs were treated with 5 μM RSV, 5 μM SRT2183, or 0.6 μM SRT1720 in the presence of M-CSF and RANKL for 6–7 days, and then the osteoclasts were fixed and stained with FITC-phalloidin to view actin belts. (B) The complete belt around the perimeter of the osteoclasts was counted. Three independent experiments were performed with ≥ 3 wells per condition. **Note:** * $p<0.05$, compared with vehicle control. Data expressed as mean ± SD.

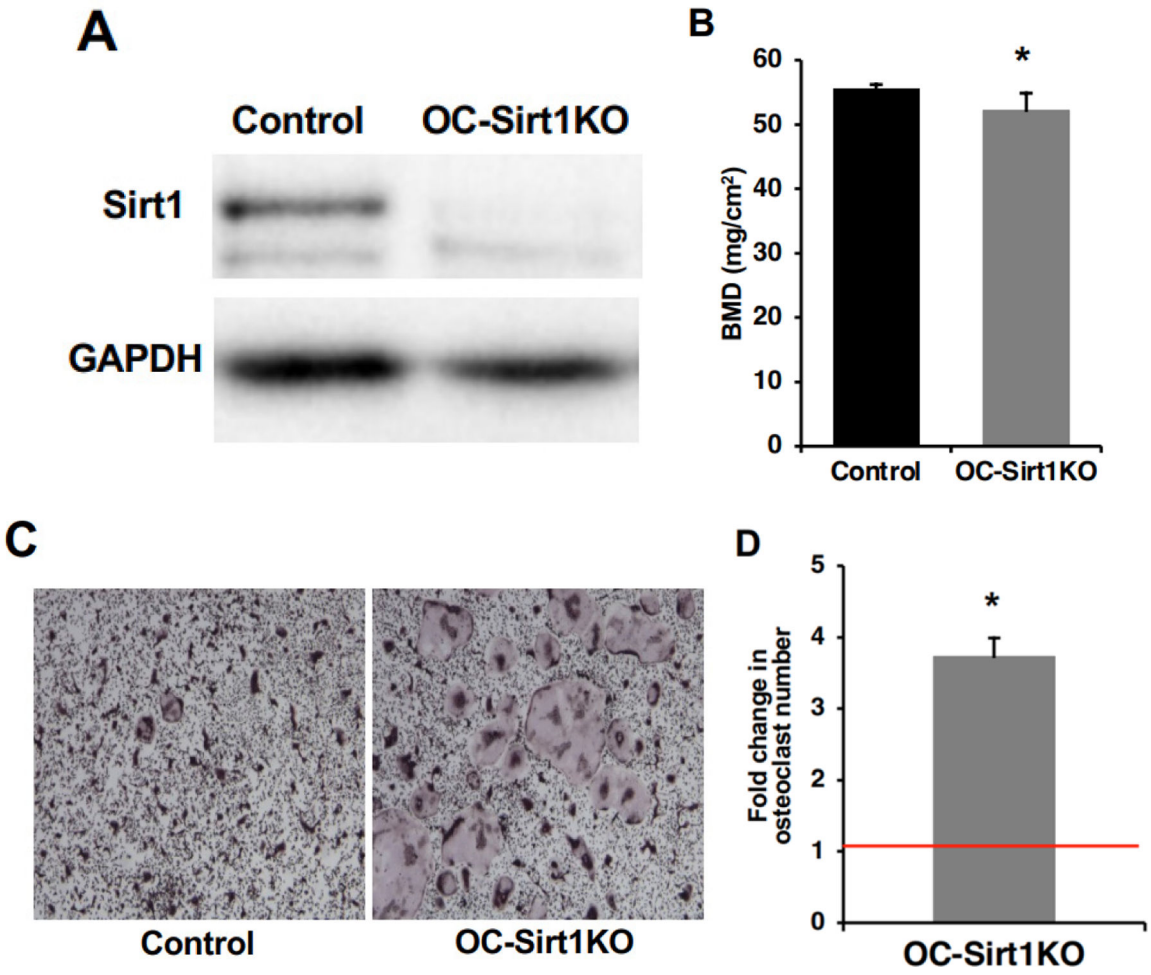

Figure 3:

Osteoclast-specific Sirt1 knockout (OC-Sirt1KO) mice exhibit low bone mineral density and a greater number of osteoclasts *ex vivo* (A) Western blot analysis of Sirt1 expression in osteoclasts derived from OC-Sirt1KO mice and littermate control mice BMCs (n=3). (B) Bone mineral density of 4-month-old male littermate control and OC-Sirt1KO mice were assessed using dual energy X-ray absorptiometry (n=6). (C) BMCs from littermate control and OC-Sirt1KO mice were treated for 6 days in the presence of 20 ng/ml M-CSF and 40 ng/ml RANKL. After 6 days, osteoclasts were fixed and stained for TRAP. (D) Osteoclasts with 3 or more nuclei were counted, and the values are represented in fold change compared to the littermate controls. Three independent experiments were performed with ≥ 3 wells per condition. **Note:** * $p<0.05$, compared with littermate control. Data expressed as mean ± SD.

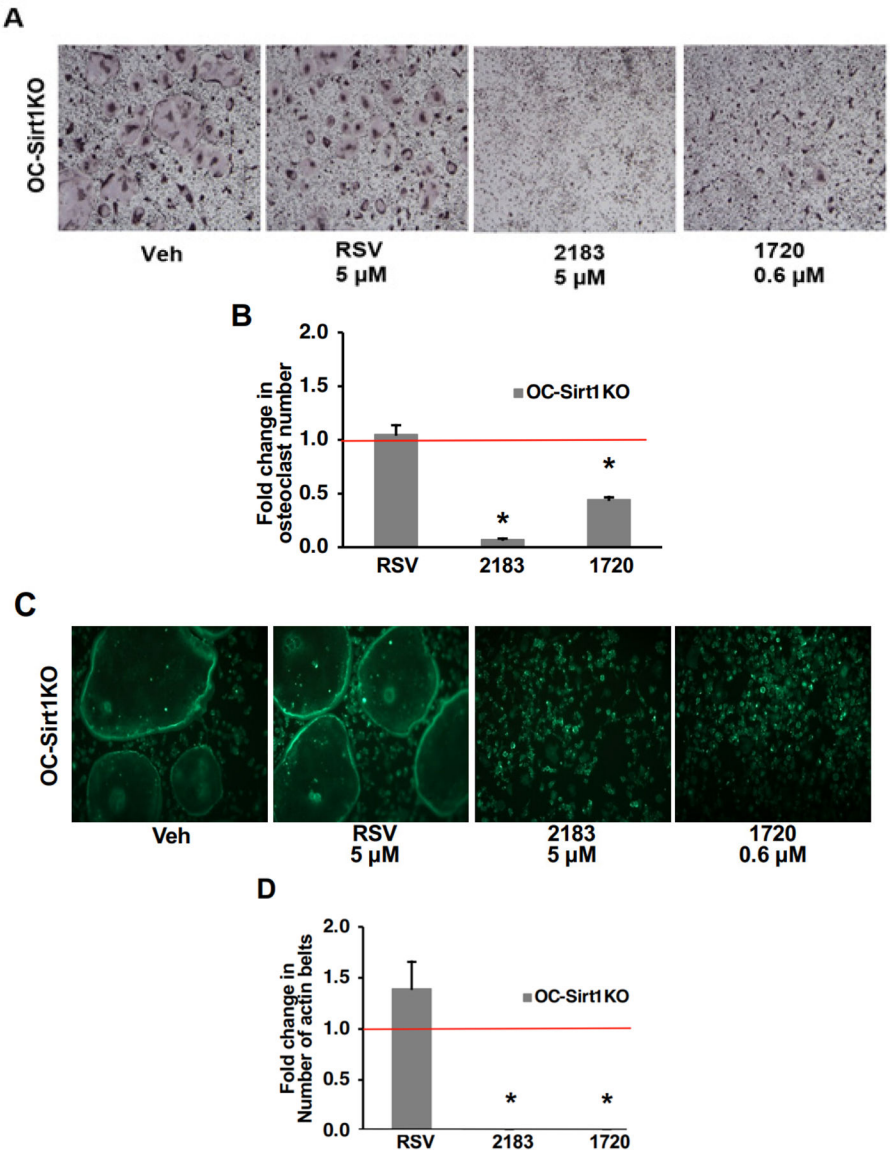

Figure 4:

SRT2183 and SRT1720 inhibit osteoclast and actin belt formation in bone marrow cells derived from OC-Sirt1KO mice BMCs from OC-Sirt1KO mice were treated for 6 days with 5 μM RSV, 5 μM SRT2183, or 0.6 μM SRT1720 in the presence of 20 ng/ml M-CSF and 40 ng/ml RANKL. After 6 days, osteoclasts were fixed and stained with TRAP (A) to count osteoclasts with 3 or more nuclei (B) or stained with FITC-phalloidin (C) to visualize and count actin belts (D). Three independent experiments were performed with ≥ 3 wells per condition. **Note:** * $p<0.05$, compared with littermate controls. Data expressed as mean ± SD.

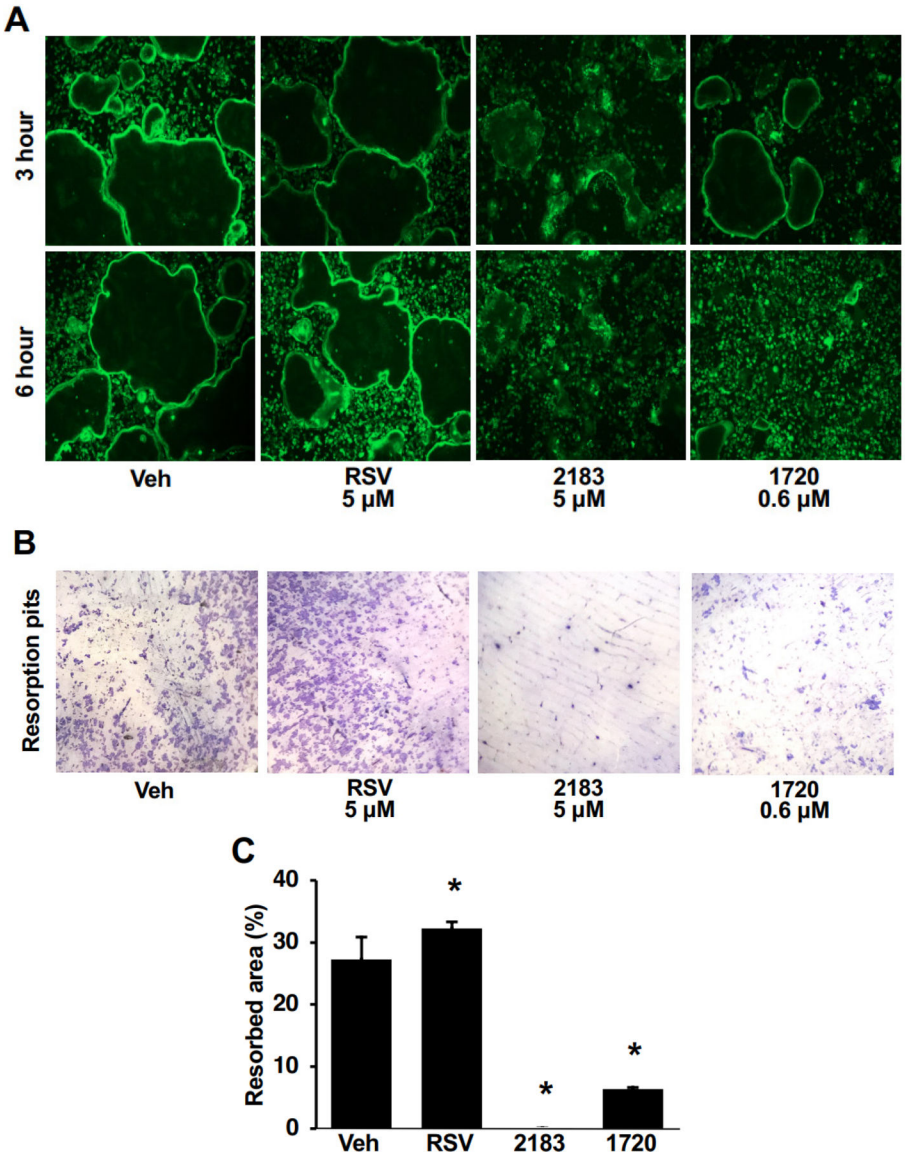

Figure 5:

SRT2183 and SRT1720 disrupt actin belts and prevent resorption in mature osteoclasts Multi-nuclear mature osteoclasts were lifted off the plate using an accutase solution and reseeded on a tissue culture plate or cortical bovine bone slices. The reseeded mature osteoclasts in the tissue culture plate were treated for 3 h and 6 h with 5 μM RSV, 5 μM SRT2183, or 0.6 μM SRT1720, then fixed and stained with FITC-Phalloidin to visualize actin belts (A). Mature osteoclasts reseeded on bone slices were treated for 72 h, and the resorption pits were visualized using 0.1% toluidine blue stain (B). The percentage of eroded area in a given bone slice was assessed using ImageJ software (C). Three independent experiments were performed with ≥ 3 wells per condition. **Note:** * $p<0.05$, compared with vehicle control. Data expressed as mean ± SD.